**Steel and Composite Structures**, *Vol. 28, No. 1* (*2018*) *25-37*
DOI: https://doi.org/10.12989/scs.2018.28.1.025



# Stability of tow-steered curved panels with geometrical defects using higher order FSM

Jamshid Fazilati *

*Aeronautical Science and Technology Department, Aerospace Research Institute, Mahestan St., Shahrek-e-gharb, Tehran, P.O. Box 14665-834, Iran*

(*Received February 24, 2018, Revised March 31, 2018, Accepted April 11, 2018*)

**Abstract.** For the first time, the parametric instability characteristics of tow-steered variable stiffness composite laminated (VSCL) cylindrical panels is investigated using B-spline finite strip method (FSM). The panel is considered containing geometrical defects including cutout and delamination. The material properties are assumed to vary along the panel axial length of any lamina according to a linear fiber-orientation variation. A uniformly distributed inplane longitudinal loading varies harmoni-cally with time is considered. The instability load frequency regions corresponding to the assumed in-plane parametric load-ing is derived using the Bolotin's first order approximation through an energy approach. In order to demonstrate the capabili-ties of the developed formulation in predicting stability behavior of the thin-walled VSCL structures, some representative results are obtained and compared with those in the literature wherever available. It is shown that the B-spline FSM is a proper tool for extracting the stability boundaries of perforated delaminated VSCL panels.

**Keywords:** parametric stability; higher order shear deformation theory; variable stiffness curved panel; cutout; delamination

## 1. Introduction

Aeronautical, space and marine structures are among main fields where both the structural weight and the overall strength are key design criteria. Nowadays, the thin-walled structures are major structural elements especially wherever the stiffness to weight ratio is a main affording issue. The stiffness to weight efficiency and in demand stiffening is also a main gain of utilizing composite reinforced laminated materials. As a result, the design and application of thin-walled plate and shell laminated composite material arrangements is a well-known field of study. The common composite designs consider constant physical lamina properties throughout entire ply area by usage of either prepreg or woven strengthening fibers. But a ply with variable mechanical properties could be achieved by changing the fiber placement characteristics for example by change in orientation angle with respect to the locality. With growing automated fiber placement technologies, it is possible to fabricate composite plies with variable fiber orientations within their geometrical domain. As a result of changing the fiber orientation angle, the ply advantages variable directional stiffness properties through the geometry surface and may be called as a variable stiffness composite laminate (VSCL).

A widespread defect of laminated structures is the ply debonding phenomenon called delamination. The delamination occurrence makes total strength reduction of the structure and activates low energy local instability and failure modes. So the estimation and calculation of the stiffness reduction effects of delamination damage on the structure's mechanical and stability behavior is of high demand. In the interior parts of the aforementioned engineering structures, the need for cable and pipe transmission or applying weight reduction design policies leads to design and application of perforated panels. The knowledge about the mechanical behavior of these type of structural elements receives high interests. During sizing design procedure of plate and shell structures under in-plane excitations, the stability becomes a critical design criterion. Under a general in-plane dynamic loading scheme, with a constant mean value and a varying harmonic part with an arbitrary loading frequency, it is possible for instability conditions to emerge called parametric or dynamic instability conditions. The excitation conditions are prevalent in case of mechanical structures as well as fluid-structural interactions.

Early reported studies on curvilinear fiber VSCL structures could be traced back to the work by Hyer and Lee (1991) on flat plates. More recently, Akhavan and Ribeiro (2011) studied the free vibration of VSCL plates made from curvilinear fibers based on a third-order shear deformation theory. An extended review on works that investigate the mechanical behavior of variable stiffness composite laminated panels is reported by Ribeiro *et al.* (2014). Their review is concerned the buckling, failure and vibrations in laminates reinforced by curvilinear fibers with some other issues also being addressed. Doubly-curved panels reinforced by curvilinear fibers are studied by Tornabene *et al.* (2016) using higher order theories. Numerical

*Corresponding author, Ph.D.,
E-mail: jfazilati@ari.ac.ir


http://www.techno-press.org/?journal=scs&subpage=6 ISSN: 1229-9367 (Print), 1598-6233 (Online)

applications based on both higher-order equivalent single layer (ESL) and layer-wise (LW) theories are presented to evaluate the curvilinear fiber influence on the static analysis by using the generalized differential quadrature (GDQ) method.

The problem of free vibration of squared and circular composite plates with delaminations around internal cutouts were concerned by Ju *et al*. (1995) by using a finite element approach. Numerical examples including composite plates with delaminations around circular holes or square cutouts were presented. It was noted that the effect of the delamination on the natural frequencies is mode-dependent while there are cases where delaminations may change the natural frequencies, even though the mode shapes are not significantly affected. Parhi *et al*. (2001) presented dynamic analysis of a squared plate with delamination. A first order shear deformation finite element formulation was utilized by employing an eight-node isoparametric element. The effects of delamination in conjunction with various boundary conditions, lay-ups and geometries were studied. Hu *et al*. (2002) studied the vibration response of moderately thick laminated plates containing delamination using a simple higher order finite element method. Two different approaches were investigated to detect a delamination in laminates. Sahu and Datta (2002) analyzed the parametric instability behavior of curved panels with cutouts subjected to in-plane static and periodic compressive edge loads by using a first order finite element method. Sanders' beside the Love's and Donnell's shallow shell theories were assumed. The effects of static and dynamic load factors, geometry, boundary conditions and the cutout geometry on the principal instability region of curved panels with cutouts were studied in detail using Bolotin's method. The effects of time variation in external pressure and material properties on the dynamic buckling time response of orthotropic cylindrical shells of variable thickness are studied by Sofiyev *et al*. (2003) by using a Galerkin approach and Ritz typr variational method. Kumar and Shrivastava (2005) developed a higher order shear deformation finite element formulation to study the free vibration response of moderately thick square composite plates with a central rectangular cutout and a delamination around the cutout. The effects of material orthotropy, boundary conditions, thickness ratio, and delamination size and location around the cutout on the free vibration response were studied. Yang and Fu (2007) examined the parametric instability of a thin-walled laminated cylinder with delamination. The Rayleigh-Ritz method and Heaviside-type displacement function technique were utilized. The problem governing Mathieu equations were solved through Bolotin's approximation method and the effects of external excitation amplitude, delamination location and size, and the material properties were studied. The free vibration analysis of laminated composite skew plates with delamination around a centrally located quadrilateral cutout is carried out by Park *et al*. (2009). The high-order shear deformation theory (HST) finite element formulation was utilized for the analysis of presence of delamination around cutout. The effect of the interactions between the skew angle and cutout size, delamination area, and length-to-thickness ratio was studied. Fazilati and Ovesy (Ovesy and Fazilati 2012, Fazilati and Ovesy 2013) developed versions of finite strip methods, namely semi-analytical and B-spline methods, based on higher order shear deformation theory and analyzed the static buckling, free vibration and parametric instability problem of longitudinally stiffened panels having rectangular internal cutouts. Two different cutout modeling approached were introduced and examined. The effects of perforations on the instability characteristics of the panels were investigated. Noh and Lee (2014) studied the parametric instability of delaminated composite skew plates under periodic in-plane loads based on the higher order shear deformation finite element method. The upper and lower boundaries of the instability regions were determined using Bolotin's method. The behavior of laminated skew plate structures with various delamination sizes, skew angle and layups beside the effect of the parametric loading on the dynamic instability regions was also analyzed. Ovesy *et al*. (2014) developed a layer-wise B-spline finite strip formulation based on first order shear deformation theory and analyzed the stability problem of laminated plates containing through the width delamination. The delamination region simulated using step displacement approximation functions. The influence of length and also the position of delamination on the buckling behavior and natural frequencies of the structure were investigated. Mohanty *et al*. (2015) investigated the parametric instability of laminated plates containing delamination internal region. A first order shear deformation finite element approach beside the Bolotin's first order approximation was utilized. Sofiyev and Kuruoglu (2015) studied the parametric instability of sandwich cylindrical shell with FG core under static and time dependent periodic axial compressive loads. The governing equations are derived using Galerkin's method based on FST Donnell's shell theory. Hirwani and coauthors (Hirwani *et al*. 2016) studied the effects of delamination on the free vibration behavior of laminated composite curved panels of different geometries. The laminated structure with seeded delamination was modelled using a higher order shear deformable finite element approach. Some experimental results were also presented for a laminated plate with different delamination size, location and positions. The effects of size, location and position of the delamination on the free vibration behavior of laminated composite shell panel has been investigated. Recently, Sofiyev *et al*. (2017) investigated the dynamic instability of truncated orthogonal FG conical shells under dynamic axial load based on FST Donnell's theory by using the Galerkin's approach. The effects of material mixture, orthotropy, and geometry on the main areas of the instability are then discussed. The dynamic behavior of variable stiffness composite laminated (VSCL) plates with curvilinear fiber orientation subjected to inplane end-loads was investigated by Fazilati (2017). The panel assumed containing internal square delamination region. B-spline finite strip method based on both classical as well as higher order shear deformation plate theories was adopted to explain the structural behavior. The effects of change in curvilinear fiber orientation angles and some model specifications on the structural stability have been studied.

The current research, for the first time, is dealing with the numerical analysis of the flat as well as moderately thick variable stiffness laminated curved cylindrical panels containing internal cutout and delamination region. A B-spline finite strip formulation is developed based on the higher order shear deformation theory in conjunction with the Koiter-Sanders theory of shallow shells. Variable stiffness due to fiber orientation variation through the longitude is considered. The static buckling, natural frequencies and parametric instability problems are concerned under uniform in-plane end loading scheme. A longitudinal uniform throughout the whole panel pre-stress loading is assumed including a constant and a time-harmonic component. The instability load frequency regions corresponding to the assumed parametric loading is derived using the Bolotin's first order approximation. The friction effects, contact conditions, and delamination growth phenomenon at delaminated interfaces and edges are overlooked. In order to demonstrate the capabilities of the developed formulation in predicting stability behavior of the thin-walled VSCL structures, some representative results are obtained and compared with those from the literature wherever available. Various examples are employed to verify the justification, accuracy and efficiency of the present novel formulation. It is shown that the B-spline FSM is a proper tool for extracting the stability boundaries of perforated and delaminated VSCL curved panels.

## 2. Formulation

A typical 3-D curved cylindrical laminated panel with a squared embedded cutout and a delamination region is considered. The delamination may be generally of either through-the-width or embedded type, with single or multiple occurrence in thickness direction. There is no limitation for the delamination either on its position or geometry. The panel laminates are stiffened using equally spaced curvilinear fibers where the fiber orientations changes linearly in the axial longitude. The geometry is divided into numbers of longitudinally adjacent cylindrical finite strips with curved crossway. Fig. 1 shows a typical panel geometry of total width $b$, length $L$ and total thickness $t$ beside a typical numerical mesh. The curved strips have length $L$ and curved width $b_s$. Typical cutout zone and embedded single delamination region are also indicated in the figure.

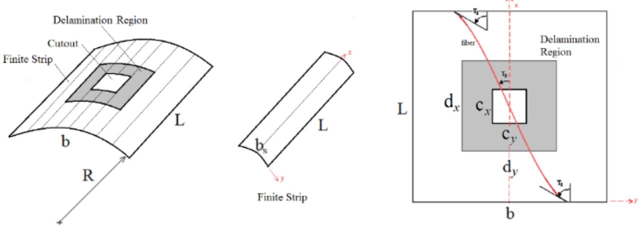


Fig. 1 Typical curved panel containing single embedded cutout surrounded by delamination with the finite strip mesh (left), typical curved finite strip (middle) and curvilinear fiber placement (right)

The displacement field inside the strip is approximated based on a Reddy-type third order shear deformation theory which assures zero shear stresses at both top and bottom surfaces of the shell and is expressed as (Fazilati and Ovesy 2013)

$$\begin{cases} u(x,y,z;t) = u^0 + \beta_x\left(z + \dfrac{-4}{3t^2}z^3\right) + \dfrac{\partial w^0}{\partial x}\left(\dfrac{-4}{3t^2}z^3\right) \\ v(x,y,z;t) = v^0\left(1 - \dfrac{1}{R}C_0 z^2 + \dfrac{8}{R}C_1 z^3\right) \\ \quad +\beta_y\left(-z - 2C_0 z^2 + C_1\left(8 - \dfrac{t^2}{R^2}\right)z^3\right) \\ \quad +\dfrac{\partial w^0}{\partial y}\left(C_0 z^2 - 8C_1 z^3\right) \\ w(x,y,z;t) = w^0 \end{cases} \tag{1}$$

$$C_0 = \frac{4}{R}\left(-24 + \frac{t^2}{R^2}\right)^{-1}, C_1 = \frac{4}{t^2}\left(-24 + \frac{t^2}{R^2}\right)^{-1}$$

Where $u$, $v$, $w$ are the displacement components of any arbitrary point, $u^0$, $v^0$, $w^0$ are the corresponding displacement components on the strip mid-surface, and $b_x$, $b_y$ are the rotations around $y$ and $x$ axis, respectively.

In the context of B-spline finite strip method, the mid-surface displacement field is approximated using series of multiplication sets of independent functions in longitudinal and crosswise directions. Series of $B_3$-splines functions are utilized in longitudinal direction while inplane linear Lagrangian functions in conjunction with out of plane third order Hermitian ones are assumed in transverse direction (Fazilati and Ovesy 2013). Any type of boundary constraints (i.e., free, simply supports, clamped) may be implemented according to the approximation displacement functions chosen.

The linear strains on cylindrical curved geometry according to Koiter-Sanders theory of shallow shells may be expressed as

$$\begin{cases} \varepsilon_x = u_{,x} \\ \varepsilon_y = v_{,y} + \dfrac{1}{R}w \\ \gamma_{xy} = u_{,y} + v_{,x} \\ \gamma_{yz} = v_{,z} + w_{,y} - \dfrac{1}{R}v \\ \gamma_{xz} = u_{,z} + w_{,x} \end{cases} \tag{2}$$

where ',' defines a differentiation operator. Substituting the displacement functions (Eq. (1)) into the strain equations (Eq. (2)), the strip strain could be expanded as

$$\begin{cases} \varepsilon_x = \varepsilon_x^{(0)} + z\varepsilon_x^{(1)} + z^2\varepsilon_x^{(2)} + z^3\varepsilon_x^{(3)} \\ \varepsilon_y = \varepsilon_y^{(0)} + z\varepsilon_y^{(1)} + z^2\varepsilon_y^{(2)} + z^3\varepsilon_y^{(3)} \\ \gamma_{xy} = \gamma_{xy}^{(0)} + z\gamma_{xy}^{(1)} + z^2\gamma_{xy}^{(2)} + z^3\gamma_{xy}^{(3)} \\ \gamma_{yz} = \gamma_{yz}^{(0)} + z\gamma_{yz}^{(1)} + z^2\gamma_{yz}^{(2)} + z^3\gamma_{yz}^{(3)} \\ \gamma_{xz} = \gamma_{xz}^{(0)} + z\gamma_{xz}^{(1)} + z^2\gamma_{xz}^{(2)} + z^3\gamma_{xz}^{(3)} \end{cases} \tag{3}$$

$$\begin{cases} \left(\varepsilon_x^{(0)},\varepsilon_y^{(0)},\gamma_{xy}^{(0)}\right) = \left(u_{,x}^0, v_{,y}^0 + \frac{1}{R}w^0, u_{,y}^0 + v_{,x}^0\right) \\ \left(\varepsilon_x^{(1)},\varepsilon_y^{(1)},\gamma_{xy}^{(1)}\right) \\ = \left(\beta_{x,x}, -\beta_{y,y}, \beta_{x,y} - \beta_{y,x} - \frac{1}{2R}\left(u_{,y}^0 - v_{,x}^0\right)\right) \\ \left(\varepsilon_x^{(2)},\varepsilon_y^{(2)},\gamma_{xy}^{(2)}\right) = \left(0, v_{,y}^*, v_{,x}^*\right) \\ \left(\varepsilon_x^{(3)},\varepsilon_y^{(3)},\gamma_{xy}^{(3)}\right) = \left(\beta_{x,x}^*, -\beta_{y,y}^*, \beta_{x,y}^* - \beta_{y,x}^*\right) \end{cases}$$

$$\begin{cases} \left(\gamma_{yz}^{(0)},\gamma_{xz}^{(0)}\right) = \left(w_{,y}^0 - \beta_y - \frac{1}{R}v^0, w_{,x}^0 + \beta_x\right) \\ \left(\gamma_{yz}^{(1)},\gamma_{xz}^{(1)}\right) = \left(2v^* + \frac{1}{R}\beta_y, 0\right) \\ \left(\gamma_{yz}^{(2)},\gamma_{xz}^{(2)}\right) = \left(-3\beta_y^* - \frac{1}{R}v^*, 3\beta_x\right) \\ \left(\gamma_{yz}^{(3)},\gamma_{xz}^{(3)}\right) = \left(\frac{1}{R}\beta_y^*, 0\right) \end{cases}, \tag{4}$$

$$\begin{Bmatrix} v^* = C_0\left(w_{,y}^0 + 2\beta_y - \frac{1}{R}v^0\right) \\ \beta_x^* = \frac{-4}{3t^2}\left(w_{,x}^0 + \beta_x\right) \\ \beta_y^* = 8C_1\left(w_{,y}^0 - \beta_y - \frac{1}{R}v^0 + \frac{t^2}{8R^2}\beta_y\right) \end{Bmatrix},$$

$$\begin{Bmatrix} C_0 = \dfrac{4}{R\left(-24 + \frac{t^2}{R^2}\right)} \\ C_1 = \dfrac{4}{t^2\left(-24 + \frac{t^2}{R^2}\right)} \end{Bmatrix}$$

The solution of the stability problem is sought through the application of the principle of virtual work. The total energy of a strip may be defined as summation of kinetic ($T$), geometrical pre-stress strain energy ($U_g$), and elastic strain ($U_e$) energy components

$$\Pi = U_e - U_g - T \tag{5}$$

The energy terms could be expressed as

$$\begin{cases} U_e = \\ \frac{1}{2}\int_{\frac{-b_s}{2}}^{\frac{b_s}{2}}\int_0^L \begin{pmatrix} \langle N\ \underline{M}\ O\ P\rangle\langle \varepsilon^{(0)}\ \varepsilon^{(1)}\ \varepsilon^{(2)}\ \varepsilon^{(3)}\rangle^T \\ +\langle Q\ R\ T\ U\rangle\langle \gamma^{(0)}\ \gamma^{(1)}\ \gamma^{(2)}\ \gamma^{(3)}\rangle^T \end{pmatrix} dx\,dy \\ U_g = \\ \frac{1}{2}t\int_{\frac{-b_s}{2}}^{\frac{b_s}{2}}\int_0^L \left(N_x\begin{bmatrix} u_{,x}^{o2} + v_{,x}^{o2} + w_{,x}^{o2} \\ +\frac{t^2}{12}\left(\beta_{x,x}^2 + \beta_{y,x}^2\right)\end{bmatrix}\right) dx\,dy \\ T = \frac{1}{2}\rho t\int_{\frac{-b_s}{2}}^{\frac{b_s}{2}}\int_0^L \begin{pmatrix} \dot{u}^{o2} + \dot{v}^{o2} + \dot{w}^{o2} \\ +\frac{t^2}{12}\left(\dot{\beta}_x{}^2 + \dot{\beta}_y{}^2\right)\end{pmatrix} dx\,dy \end{cases} \tag{6}$$

With denoting of an unchanged material mass density as $\rho$, differentiation with respect to time as upper dot and a matrix transpose operator as superscript $T$. The force resultants ($N$, $\underline{M}$, $O$, $P$, $Q$, $R$, $T$, $U$) are location dependent due to change in the fiber orientation angles on all plies and can be related to the strain terms via the curvilinear fiber laminated material equivalent stiffness matrices through: (Fazilati and Ovesy 2013)

$$\begin{gathered} \begin{Bmatrix} \{N\} \\ \{\underline{M}\} \\ \{O\} \\ \{P\} \end{Bmatrix} = \begin{bmatrix} [A] & [B] & [D] & [E] \\ [B] & [D] & [E] & [F] \\ [D] & [E] & [F] & [I] \\ [E] & [F] & [I] & [H] \end{bmatrix}_{(x,y)} \begin{Bmatrix} \{\varepsilon^{(0)}\} \\ \{\varepsilon^{(1)}\} \\ \{\varepsilon^{(2)}\} \\ \{\varepsilon^{(3)}\} \end{Bmatrix}, \\ \begin{Bmatrix} \{Q\} \\ \{R\} \\ \{T\} \\ \{U\} \end{Bmatrix} = \begin{bmatrix} [A^S] & [B^S] & [D^S] & [E^S] \\ [B^S] & [D^S] & [E^S] & [F^S] \\ [D^S] & [E^S] & [F^S] & [I^S] \\ [E^S] & [F^S] & [I^S] & [H^S] \end{bmatrix}_{(x,y)} \begin{Bmatrix} \{\gamma^{(0)}\} \\ \{\gamma^{(1)}\} \\ \{\gamma^{(2)}\} \\ \{\gamma^{(3)}\} \end{Bmatrix} \end{gathered} \tag{7}$$

Applying a longitudinal uniform loading scheme as superposition of a constant (static) component beside a harmonically changing (dynamic) one

$$N_x = a^S N_{cr} + a^D N_{cr}\cos(\omega t) \tag{8}$$

where $w$, $a^S$, $a^D$ and $N_{cr}$ are the exciting load frequency, unchanged loading component coefficient, varying loading component coefficient, and the static buckling load of the panel, respectively. Substituting of the strain and force resultants and loading scheme in energy integral Eq. (6), integrating the energies throughout the strip area, minimizing the energy equilibrium Eq. (5), factorizing with respect to the degrees of freedom vector, and some further handlings including assembling the strip equations and implementing of necessary boundary conditions, the governing equation of the parametric instability of the VSCL curved panel will be obtained and simplified as

$$M\ddot{\delta} + \left(K - a^S K_g^S\right)\delta - a^D K_g^D\,cos(\omega t)\,\delta = 0 \tag{9}$$

Where $M$, $K$, $K_g{}^S$, and $K_g{}^D$ are the global structural matrices corresponding respectively to kinetics energy, elastic strain energy and geometrical prestress energies corresponding to static and dynamic components of loading. $d$ is the global vector of unconstrained degrees of freedom. By implementing of the Bolotin's first order approximation corresponding to excitation frequency of twice the fundamental frequency of the model, which gives more critical conditions, the time varying vector, $d$, may be approximated as

$$\delta = A\sin\left(\frac{1}{2}\omega t\right) + B\cos\left(\frac{1}{2}\omega t\right) \tag{10}$$

With time-independent coefficient vectors, $A$ and $B$, which are called degrees of freedom vectors. Substitution of Eq. (10) into Eq. (9), factorization of harmonic terms and setting their coefficients to zero leads to a set of homogenous equations. For a non-trivial solution of unknown degrees of freedom vectors, $A$ and $B$, the determinants of the coefficient matrices should be set to zero. The governing Eq. (9) is then reduced to two subsequent eigenvalue problems as

$$\begin{cases} \left(K - a^S K_g^S + \frac{1}{2}a^D K_g^D\right) - \frac{1}{4}\omega^2 M = 0 \\ \left(K - a^S K_g^S - \frac{1}{2}a^D K_g^D\right) - \frac{1}{4}\omega^2 M = 0 \end{cases} \tag{11}$$

Those equations are corresponding to vectors $A$ and $B$ and could be solved separately. The solution process reveals two boundaries of the instability region of the structure in terms of loading parameter sets of ($a^S$, $a^D$, $w$). It is to be remarked here that the governing Eq. (9) in case of time independent conditions (i.e., zero dynamic loading) would reduce to a well-known static buckling equation. Furthermore, in case when no loading exists, the equation reduces to a free vibration problem governing equation. The frequencies and mode shapes in all types of problems may be extracted by utilizing a QR eigenvalue decomposition algorithm.

Effects of existence of any defect including either cutout or delamination on the structural behavior and its governing equation may be taken into account by employing proper techniques. The modeling of the cutout defect is formulated through using the "Negative stiffness approach" as is completely characterized previously in (Ovesy and Fazilati 2012). In this approach a perfect numerical model is utilized and the effects of the cutout is established through excluding the cutout zone from the energy integrations intervals of Eq. (6).

The technique for modeling the delamination effects is through using multiple numerical models of the same geometry but different in the through-thickness definitions. In the delamination region, the plate is actually a set of two tangent separate thinner surfaces. To bring a single delamination defect into consideration, the main idea is to use double strips in the thickness direction in order to separately simulate two surfaces. This means that the whole plate or shell is numerically modeled as composition of two analogous layers of strip meshes with dissimilar lay-ups characteristics. Inside the delamination zone, the two layers are unconnected while out of the delamination zone, all of degrees of freedom of the two layer must rigidly linked to each other via knots' merging process. The corresponding strips in upper and lower layers have the same geometrical and numerical characteristics but are different in layup. According to Fig. 2, the strip knots of the same planar positions are merged together in all the perfect panel areas and also at the edges of the delamination zone. So, it is necessary to have knots placed on the edges of the delamination region. This approach could also be generalized for the case of a geometry with $N$ delamination in thickness direction with defining $N + 1$ separate tangent layers. Every strip layer has the same geometry properties but are different in bending stiffness. To fulfill the true bending properties of every layer in a strip with respect to the plate mid.-surface, every layer lay-up is considered similar to the whole plate layup with the redundant layers' material changed to a null, stiff-less and weight-less one as is shown in Fig. 2. These consideration guarantees the physical conditions at the edges of the delamination zone.

As a variable stiffness ply, it is assumed that the fiber orientation angle changes linearly along the axial direction of the strip geometry. The changing fiber angle is denoted by a two-angle set $<T_0, T_1>$ where the former one and the latter represent the fiber angle at the strip's middle length and the strip's two ends, respectively (Fazilati2017). Diagram of Fig. 1 depicts the typical changing fiber orientation scheme. The fiber angle at every arbitrary point in the geometry may be expressed by the following linear equation

$$\theta(x) = T_0 + \frac{|x - L/2|}{L/2}(T_1 - T_0), \quad 0 < x < L \qquad (12)$$

## 3. Results and discussion

In this section the results of some representative structural stability problems of curved VSCL panels containing cutout and delamination defects are extracted using the developed higher order finite strip method and compared with some available in the literature. Some parametric studies are also provided using the developed numerical tool.

An isotropic square cylindrical panel containing a central square perforation is considered with all edges clamped. The cutout area is 25% of total panel area. The geometry specifications as well as material properties are given as follows

$$\begin{cases} E = 68.796GPa \ , \upsilon = 0.3 \ , \ \rho = 2720\ kgm^{-3} \\ L = b = 0.5\ m \ , \quad \dfrac{L}{t} = 250 \ , \quad \dfrac{L}{R} = 0.25 \\ c_x = c_y = c \ , \quad \dfrac{c}{L} = 0.5 \\ d_x = d_y = c \ \ (no\ delamination) \end{cases} \qquad (13)$$

The convergence study on first four natural frequencies of the panel is performed by using the higher order FSM and compared with the results reported by Sahu and Datta (2002) and Sivasubramonian *et al.* (1999). Table 1 presents the convergence of the calculated FSM results with increase in number of strips. The spline FSM frequencies are

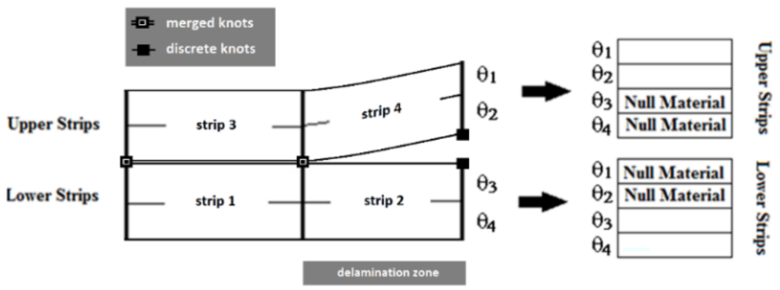


Fig. 2 Delamination modeling approach overview for a mid-thickness delamination on typical four-layer laminate

Table 1 First four natural frequencies in Hz for full clamped isotropic curved panel with central square cutout (no delamination)

| Method | Strips | Mode I | Mode II | Mode III | Mode IV |
|---|---|---|---|---|---|
| Present FSM | 16 | 207.66 | 213.84 | 317.07 | 355.35 |
| | 20 | 198.77 | 203.59 | 309.68 | 337.57 |
| | 24 | 194.28 | 198.51 | 306.49 | 330.17 |
| | 28 | 191.63 | 195.54 | 304.81 | 326.39 |
| | 32 | 190.01 | 193.75 | 303.86 | 324.38 |
| FST* FEM (Sahu and Datta 2002) | | 184.73 | 187.52 | 295.68 | 310.3 |
| FEM (Sivasubramonian *et al*. 1999) | | 185.3 | 188.2 | 295.9 | 309.7 |

* FST: first order shear deformation theory

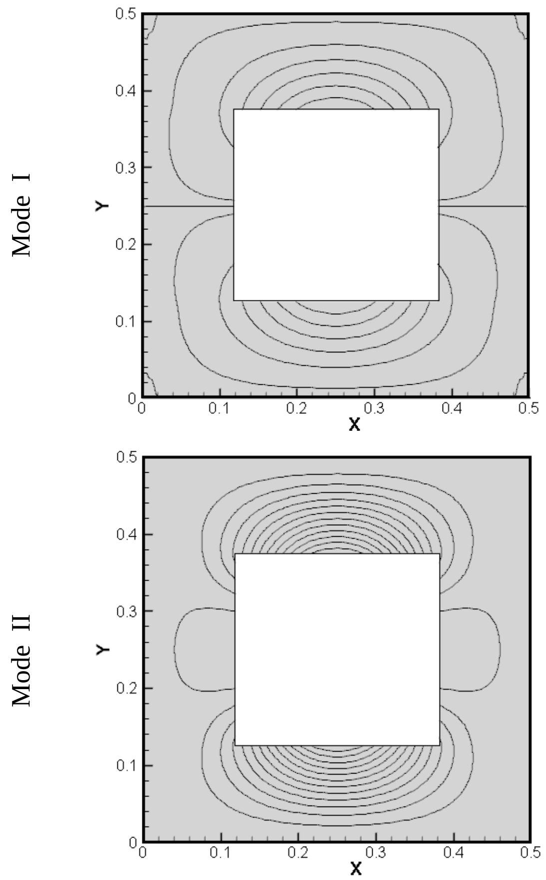


Fig. 3 First two free vibration mode shapes of the perforated curved panel

relatively in good agreement compared to those extracted from FEM. The two first free vibration mode shapes of the perforated curved panel are also acquired and plotted in Fig. 3.

A squared flat laminated plate containing a central square cutout is considered. A 40-layer lay-up of $[(\pm45/0_2)_3(90/0_2/90)_2]_S$ is assumed and simply supported end constraints are applied. The square cutout located at the center of the panel with edge fractions of ($c/L$) 0, 0.2 and 0.4. The orthotropic ply material properties and panel geometry specifications are

$$\begin{cases} E_1 = 130\ GPa,\ \ v_{12} = 0.35,\ \ \rho = 1500\ kgm^{-3} \\ \dfrac{E_1}{E_2} = 13,\ \ \dfrac{G_{12}}{E_2} = 0.5,\ \ \dfrac{G_{23}}{E_2} = 0.33 \\ L = b = 0.45\ m,\ \ \dfrac{L}{t} = 75,\ \ \dfrac{L}{R} = 0 \\ c_x = c_y = c,\ \ \dfrac{c}{L} = 0.0; 0.2; 0.4 \\ d_x = d_y = c\ \ (no\ delamination) \end{cases} \tag{14}$$

The first four natural frequencies of the perforated laminated plate are extracted using the HST-FSM formulation and are compared with those from the first order shear deformation theory (FST) as well as third order shear deformation theory (HST) finite element formulations of Kumar and Shrivastava (2005) and Park *et al*. (2009) as given in Table 2. The results show a very good accuracy of HST-FSM calculations in comparison with results from the literature. It is notable that the natural frequency of the panel with larger cutout is higher than the perfect panel but for the case of higher more complex modes, larger cutout area corresponds with lower frequencies.

The same laminated flat panel is considered with central cutout and a delamination region surrounding the perforation. A central square cutout of size ($c/L$) 0.1 is considered while surrounded by delamination with width fractions ($(d-c)/2L$) of 0, 0.1 and 0.2. The results presented in Table 3 shows a very good accuracy of FSM calculations in comparison with reported ones.

In the remainder of this section, some parametric studies are performed on the effects of different geometrical as well as lay-up specifications on the panel's static as well as dynamic instability criteria. The parameters under investigation are involving variable fiber orientation lay-ups, delamination region area, panel curvature, and delamination position in the laminate thickness. The assumed typical geometry specifications could be summarized as

$$\begin{cases} L = b = 1.0m,\ L/t = 10 \\ L/R = 0.0/0.25/0.5/1.0/2.0/4.0 \\ c_x = c_y = c,\ c/L = 0.1 \\ d_x = d_y = d,\ (d-c)/L = 0.0/0.1/0.3/0.5/0.7 \end{cases} \tag{15}$$

Table 2 Normalized first four natural frequencies for simply supported square flat laminate with different central square cutout sizes without delaminations ($w = \omega b^2/(h\sqrt{E_2/\rho})$

| | | Present FSM | FEM (Kumar and Shrivastava 2005) | FEM (Kumar and Shrivastava 2005) | FEM (Park *et al*. 2009) | FEM (Park *et al*. 2009) |
|---|---|---|---|---|---|---|
| *c*/*L* | Mode | (HST) | (FST) | (HST) | (FST) | (HST) |
| 0 | 1 | 13.58 | 13.59 | 13.71 | 13.68 | 13.59 |
| | 2 | 29.07 | 29.11 | 29.5 | 29.89 | 29 |
| | 3 | 37.63 | 37.79 | 38.3 | 39.1 | 37.66 |
| | 4 | 53.70 | 53.93 | 54.85 | 55.56 | 53.6 |
| 0.2 | 1 | 13.28 | 13.15 | 13.4 | 13.16 | 13.11 |
| | 2 | 28.44 | 28.39 | 29.06 | 29.21 | 28.24 |
| | 3 | 36.98 | 35.79 | 36.9 | 37.15 | 35.52 |
| | 4 | 52.29 | 52.4 | 53.42 | 53.88 | 51.96 |
| 0.4 | 1 | 14.10 | 14.24 | 14.86 | 14.22 | 14.17 |
| | 2 | 26.05 | 25.65 | 26.68 | 26.21 | 25.64 |
| | 3 | 28.72 | 28.64 | 29.91 | 29.38 | 28.6 |
| | 4 | 48.64 | 48.71 | 49.76 | 50.18 | 48.26 |

Table 3 Normalized first four natural frequencies for simply supported square flat laminate with central square cutout and different delamination sizes. ($w = \omega b^2/(h\sqrt{E_2/\rho})$

| | | Present FSM | FEM (Kumar and Shrivastava 2005) | FEM (Kumar and Shrivastava 2005) | FEM (Park *et al*. 2009) |
|---|---|---|---|---|---|
| (*d* – *c*) / 2*L* | Mode | (HST) | (FST) | (HST) | (HST) |
| 0 | 1 | 13.53 | 13.60 | 13.40 | 13.401 |
| | 2 | 29.28 | 29.57 | 29.07 | 29.062 |
| | 3 | 37.60 | 38.33 | 37.65 | 37.583 |
| | 4 | 53.59 | 54.51 | 53.51 | 53.832 |
| | 5 | 55.18 | 55.41 | 55.08 | -- |
| | 6 | 76.39 | 78.51 | 78.16 | -- |
| 0.1 | 1 | 13.52 | 13.41 | 13.35 | 13.272 |
| | 2 | 28.35 | 28.98 | 28.04 | 27.972 |
| | 3 | 35.14 | 36.33 | 34.86 | 35.184 |
| | 4 | 53.35 | 54.36 | 52.84 | 53.805 |
| | 5 | 54.85 | 54.08 | 53.54 | -- |
| | 6 | 74.40 | 77.79 | 74.92 | -- |
| 0.2 | 1 | 13.37 | 13.26 | 13.25 | 12.984 |
| | 2 | 25.08 | 25.71 | 25.01 | 25.421 |
| | 3 | 28.43 | 29.44 | 28.32 | 28.938 |
| | 4 | 47.67 | 49.07 | 46.9 | 44.159 |
| | 5 | 48.23 | 49.47 | 47.72 | -- |
| | 6 | 49.96 | 61.97 | 49.86 | -- |

The panel is laid-up from 4 or 8 layers of variable stiffness plies. The ply orthotropic material properties are assumed as follows

$$\begin{cases} E_1 = 130GPa \ , \ E_1/E_2 = 13 \ , G_{12}/E_2 = 0.5 \\ G_{23}/E_2 = 0.33, \ \upsilon_{12} = 0.35 \ \ , \rho = 1500\,kgm^{-3} \end{cases} \tag{16}$$

### 3.1 Effects of fiber angle variation

A fully-simply supported four-layer VSCL curved panel is considered containing an internal central square cutout and a central mid-thickness delaminated region. A length to radius ratio (*L*/*R*) of 1.0, cutout size ratio (*c*/*L*) of 0.2 and mid-thickness delamination size ratio ((*d*-*c*)/*L*) of 0.3 is

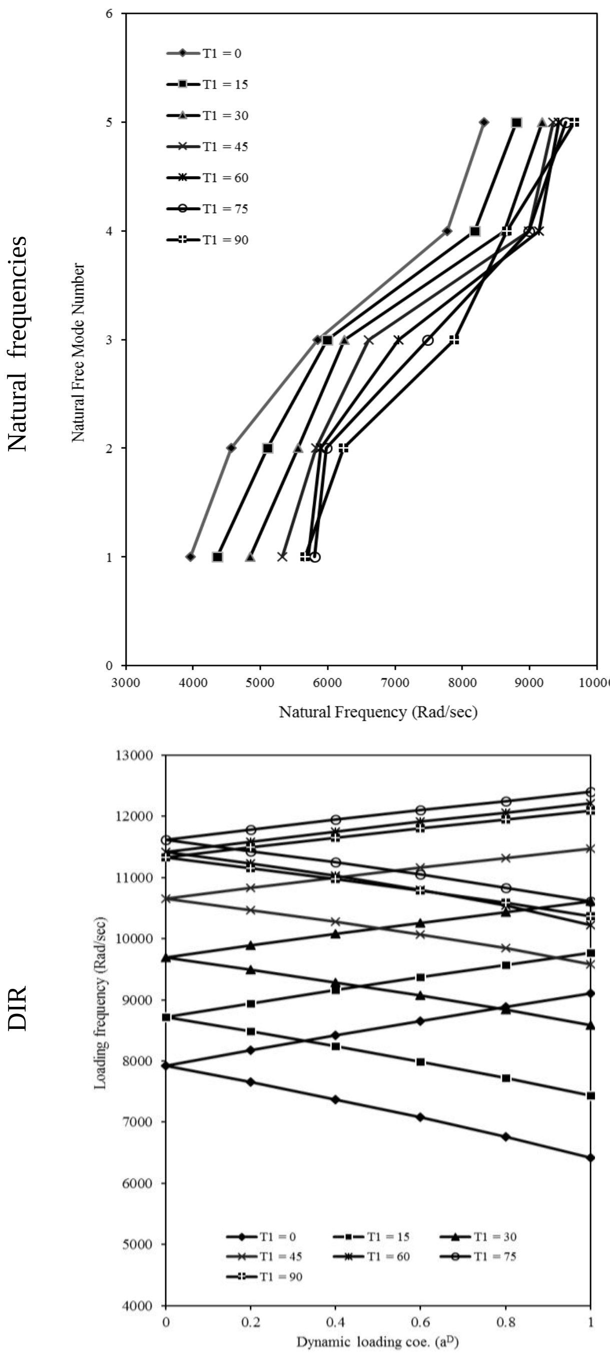


Fig. 4 Natural frequencies (up) and DIR (down) of simply supported curved VSCL panel with layup [± < 45, $\theta$ >]$_S$ ($a^s$ = 0)

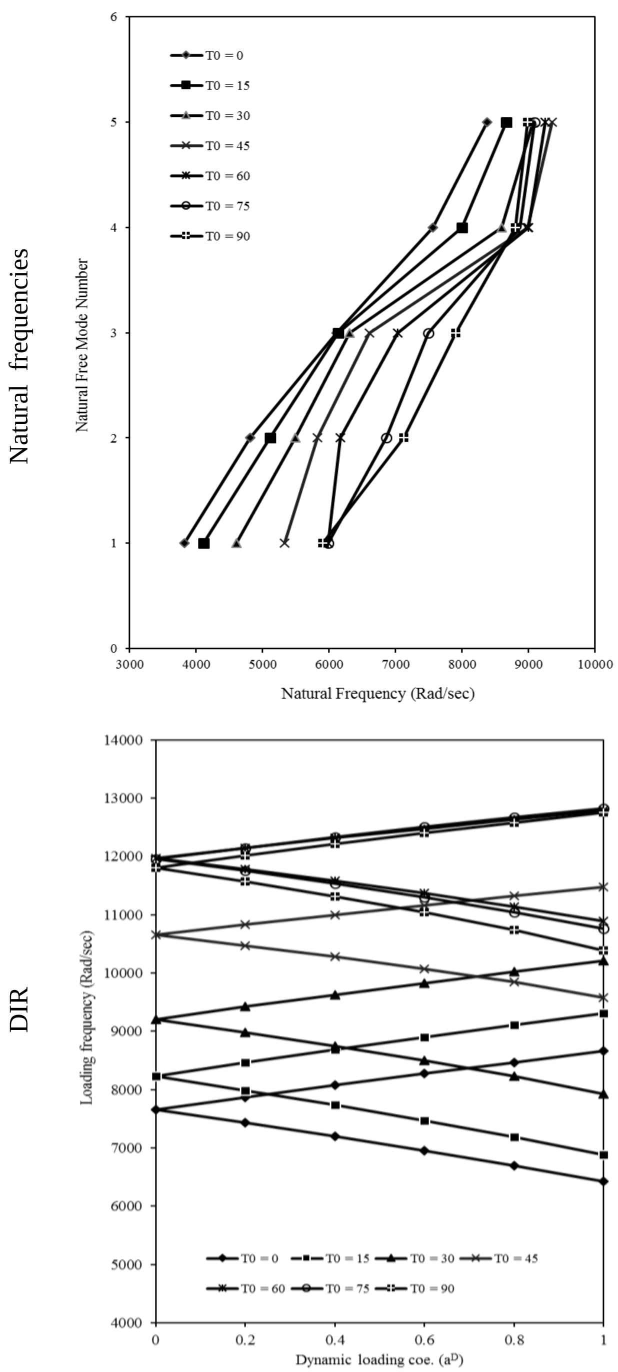


Fig. 5 natural frequencies (left) and DIR (right) of simply supported curved VSCL panel with layup [± < $\theta$, 45>]$_S$ ($a^s$ = 0)

assumed. The plies are assumed strengthened using curvilinear fibers where either middle-length angle ($T_0$) or end angles ($T_1$) is kept unchanged and the other alters. The fixed fiber angle is taken 45 degrees with respect to the longitude. The study on the first five natural frequencies as well as dynamic instability regions (DIR) under uniform longitudinal excitations are performed while ply layups varies. Fig. 4 depicts the results for change in natural frequencies and DIR of the panel with frozen middle-length angle but different end fiber angles of [± < 45, $\theta$ >]$_S$. The results show that the stability characteristics of the laminate improves as the end fiber angle increases. But it is also notable that the maximum stability (high natural frequency and high-frequency instability region) are obtained in case of layup [± < 45, 75 >]$_S$, i.e., the tow-steered layup with middle-length angle 45 and end fiber angles of 75.

Fig. 5 presents natural frequencies and DIR changes as the middle-length angle variates and the end fiber angle is fixed at 45. The uppermost stability of the laminate is obtained for the case of [± < 60, 45 >]$_S$ and [± < 75, 45 >]$_S$ layups while the worst instability characteristics are observed for $T_0$ = 0. A sample fundamental vibration mode shape of the perforated curved VSCL panel with

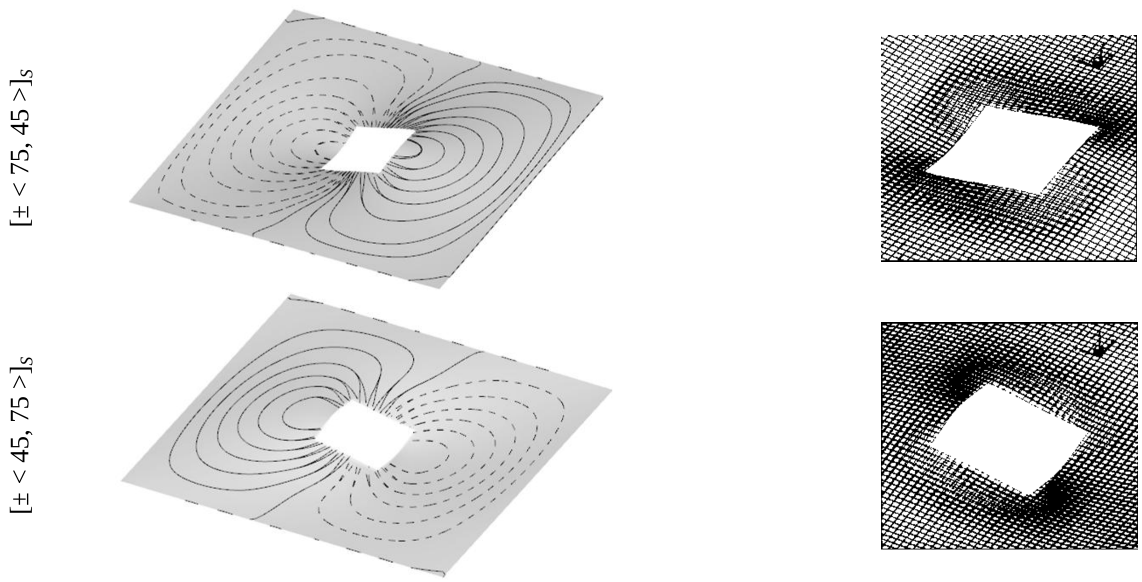


Fig. 6 The fundamental vibration mode shape of curved VSCL panel with cutout and delamination

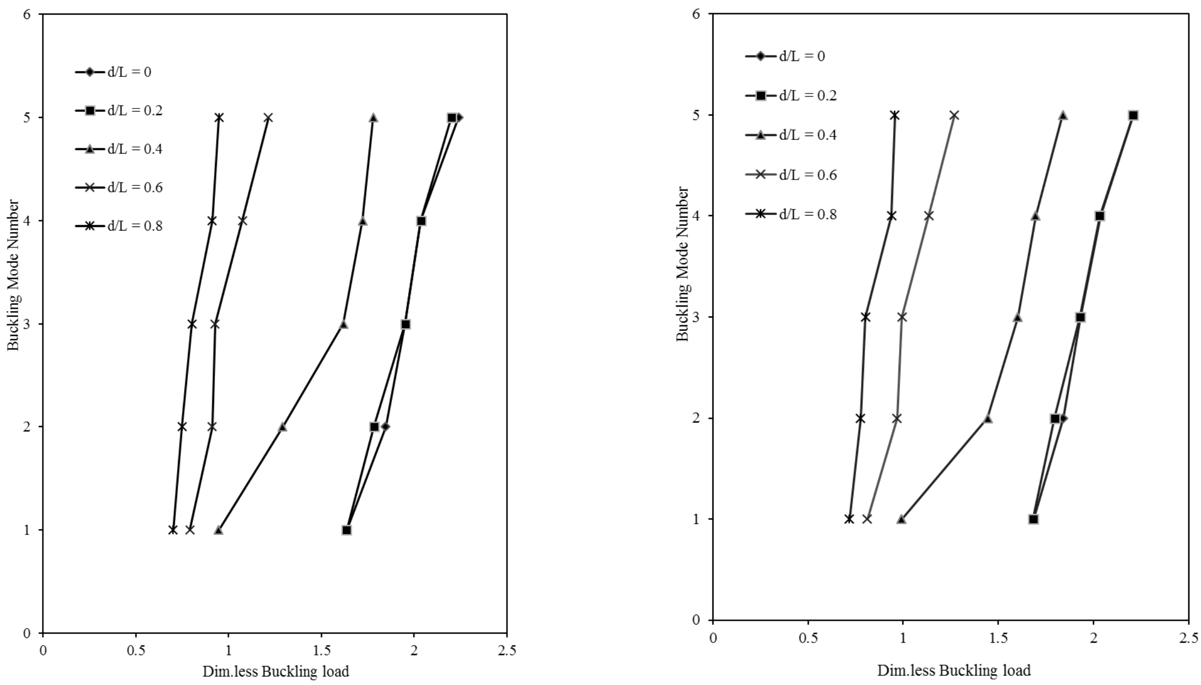


Fig. 7 The first five critical buckling load ratio ($\sigma_{cr}/E_2$) of perforated VSCL curved panel with different delamination areas [$\pm<60, 45>]_S$ (left), [$\pm<45, 60>]_S$ (right)

delamination is illustrated in Fig. 6 where the opening of the delamination region is noticeable.

### *3.2 Effects of change in delamination size*

The same fully-simply supported four-layer VSCL curved panel with layups [$\pm<45, 60>]_S$ and [$\pm<60, 45>]_S$ are considered with an embedded central square cutout and central delaminated regions of different areas. A length to radius ratio ($L/R$) of 1.0, cutout length ratio ($c/L$) of 0.1 and mid-thickness delamination size ratios ($d/L$) of 0.1, 0.2, 0.4, 0.6, and 0.8 (equal to $(d\text{-}c)/L$ ratios of 0.0, 0.1, 0.3, 0.5, and 0.7) are assumed. Illustrations of Figs. 7-9 show the stability properties of the perforated curved VSCL panel with different central delamination region sizes. The study on the buckling critical load, natural frequencies and dynamic instability regions under uniform longitudinal excitations shows that a delamination region smaller than 0.2 edge ratio could not noticeably affect the stability properties of the curved panel. But wider delaminations can primarily weaken the stability behavior. This reduction especially affects the static instability (buckling) and load tolerating characteristics. Furthermore, the panel with higher $T_0$, i.e., 60, provides the most stable design layup.

### 3.3 Effects of curvature

The panel layups $[\pm\langle 45, 60\rangle]_S$ and $[\pm\langle 60, 45\rangle]_S$ are considered with an internal central square cutout and an edge delaminated region. The panel curvature ratio ($L/R$) is varied from 0.0. to 4.0 while a constant cutout edge ratio ($c/L$) of 0.1 and mid-thickness delamination edge ratio ($(d-c)/L$) of 0.1 are assumed. The extracted results for critical buckling load, natural frequencies and dynamic instability regions of perforated VSCL panel with different curvatures and lay-ups are presented in Figs. 10, 11, and 12, respectively. The study on the buckling critical load, natural frequencies and dynamic instability regions under uniform longitudinal excitations shows that the curved panels are more stable than a flat panel both statically and dynamically. In case of a lower radius of curvature, the dynamic instability region of the panel shifts toward higher loading frequencies with meaning-less changes in the instability region size. This means that higher curvatures (with lower radius) makes the panel more stable. The results depicted in figures shows that the curvature effects is more considerable in layup $[\pm\langle 60, 45\rangle]_S$.

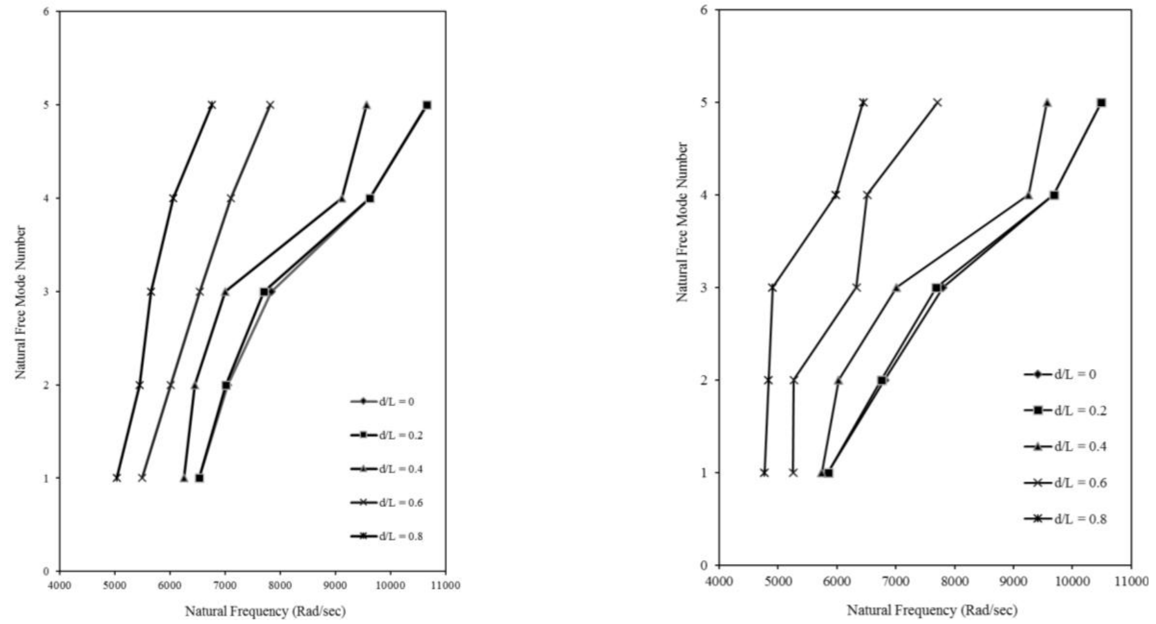


Fig. 8 The first five natural frequencies of perforated VSCL curved panel with different delamination areas $[\pm\langle 60, 45\rangle]_S$ (left), $[\pm\langle 45, 60\rangle]_S$ (right)

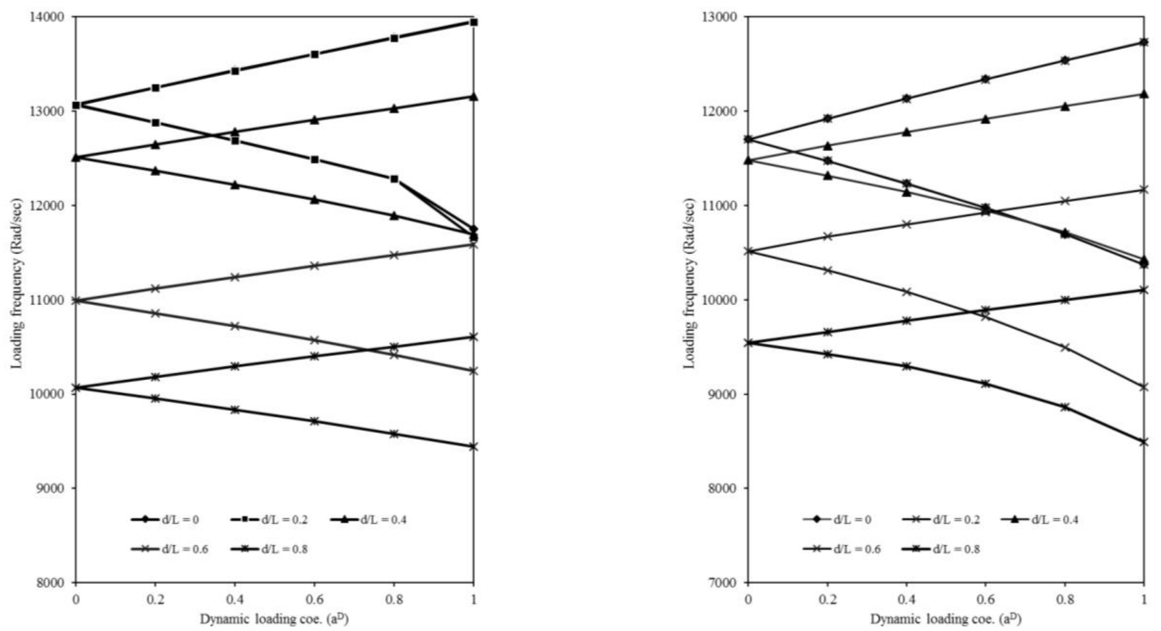


Fig. 9 The dynamic instability regions of perforated VSCL curved panel with different delamination areas $[\pm\langle 60, 45\rangle]_S$ (left), $[\pm\langle 45, 60\rangle]_S$ (right)

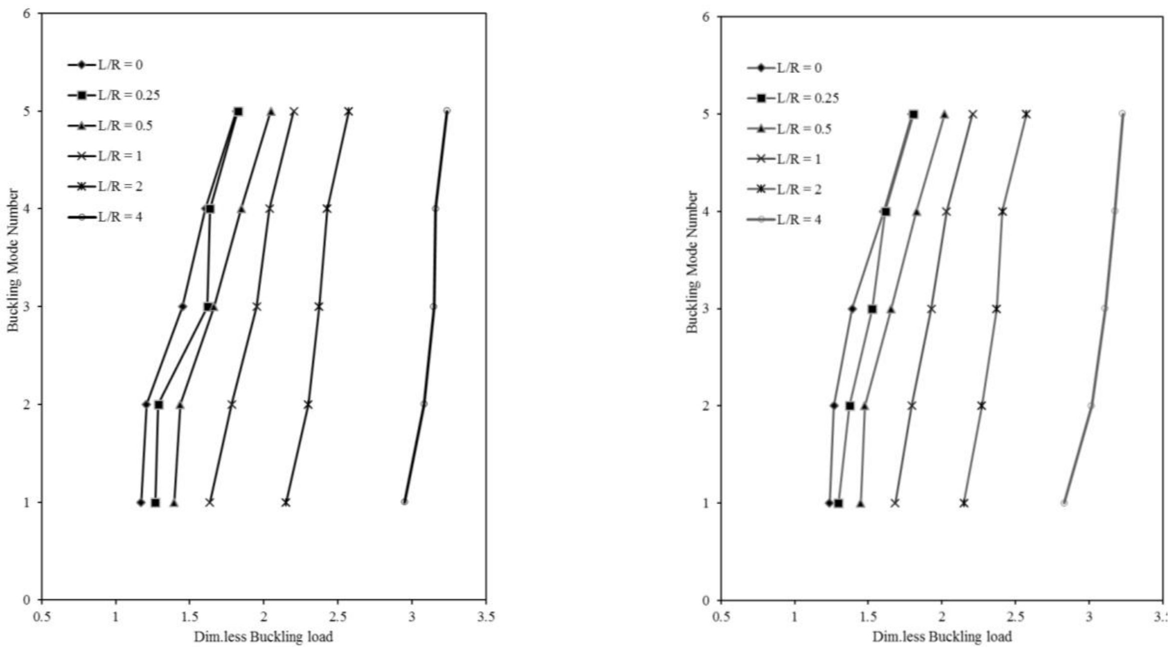


Fig. 10 The first five critical buckling load ratios ($\sigma_{cr}/E_2$) of perforated VSCL panel with different curvatures $[\pm<60, 45>]_S$ (left), $[\pm<45, 60>]_S$ (right)

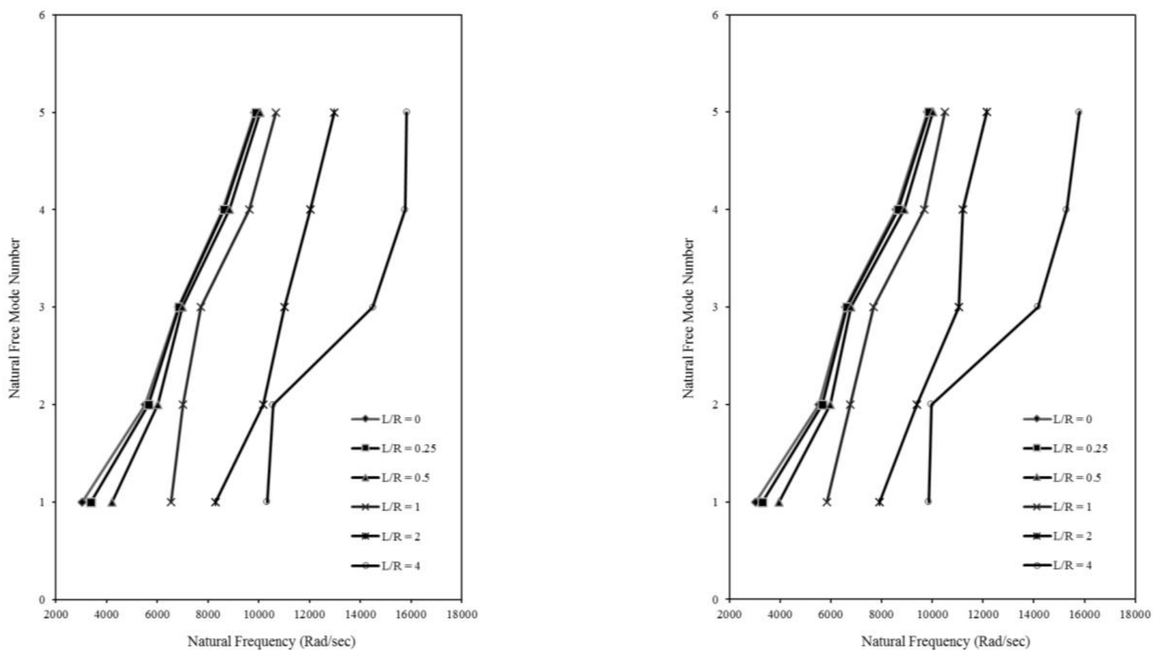


Fig. 11 The first five natural frequencies of perforated VSCL panel with different curvatures $[\pm<60, 45>]_S$ (left), $[\pm<45, 60>]_S$ (right)

### *3.4 Effects of delamination location*

Finally a simply supported perforated curved VSCL panel with 8-layer layup $[\pm<60, 45>]_S$ is considered and the effects of change in the delamination position through the laminate thickness is examined. The panel curvature ratio ($L/R$) is kept fixed at 1.0 along with a cutout edge ratio ($c/L$) of 0.1 and delamination edge ratio ($(d\text{-}c)/L$) of 0.3. The square central delamination region is considered in the mid-thickness beside three through the thickness possible positions.

Fig. 13 shows the first five natural frequencies as well as DIR of the curved panel with altered delamination positions through the thickness. Results show that the change of the delamination position has limited effects on the reduction of natural frequencies especially in first mode. But a delamination located at higher position levels reduces the load tolerance of the structure. It is also shown that the dynamic instability regions of the panel are not changed in base frequencies when the delamination travels towards the

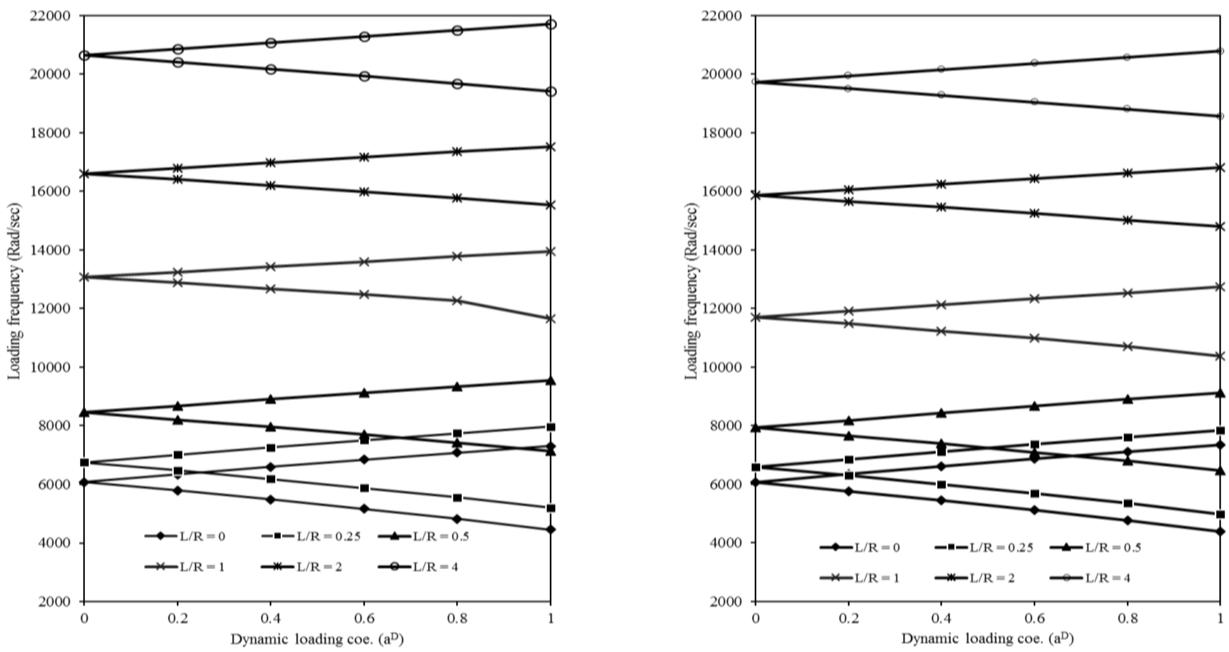


Fig. 12 the dynamic instability regions of perforated VSCL panel with different curvatures $[\pm < 60, 45 >]_S$ (left), $[\pm < 45, 60>]_S$ (right)

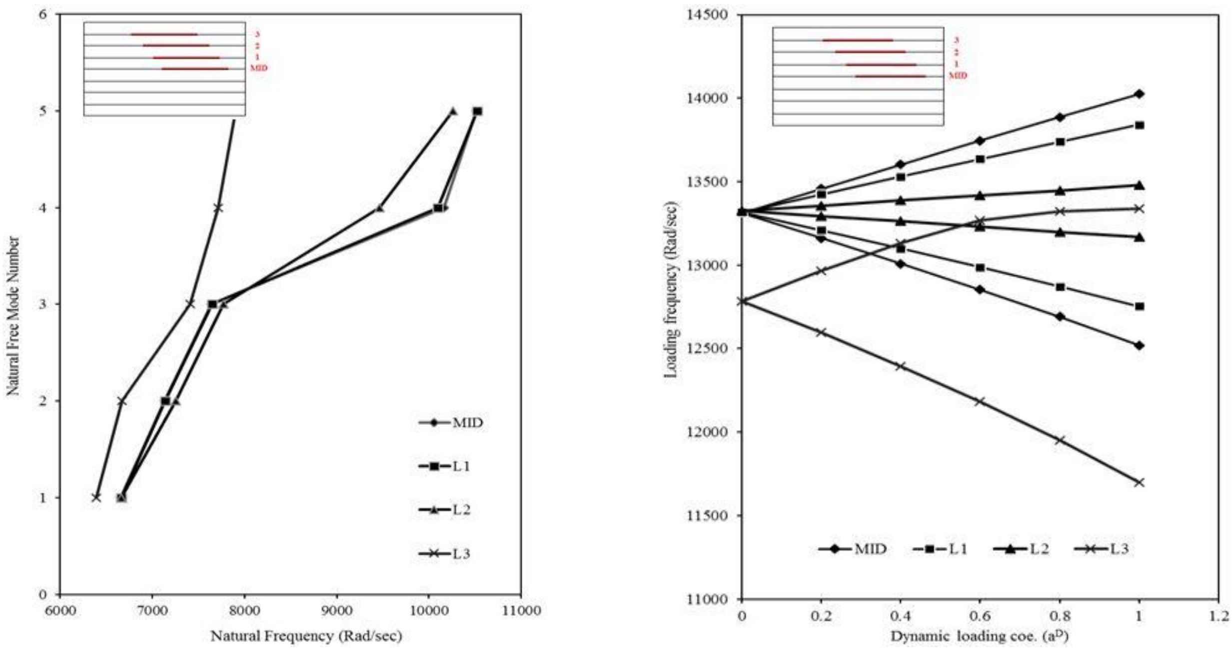


Fig. 13 The natural frequencies (left) and dynamic instability regions (right) of perforated VSCL panel with change in delamination through the thickness positions

upper position, but it is also notable that a delamination at position 1 or 2 provides a narrower DIR zone which means a more limited instability. A delamination in position 3, instead, shows reduction in natural frequency and more critical DIR as well.

## 4. Conclusions

The research is dealing with the numerical analysis of the flat as well as curved cylindrical moderately thick laminated panels containing internal perforation and rectangular delamination region. The panel is assumed made from layered variable stiffness lamina (VSCL) where the material properties are varied according to a linear fiber orientation angle function along the longitude. An enhanced B-spline finite strip formulation is developed based on the higher order shear deformation theory and the Koiter-Sanders theory of shallow cylindrical shells. The static buckling, natural frequencies and parametric instability problems are concerned under uniform inplane harmonic end-loading scheme. A longitudinal uniform through the whole panel pre-stress loading is assumed consisting of a constant as well as time-harmonic component. The instability load frequency regions corresponding to the assumed in-plane parametric loading is derived using the Bolotin's first order approximation. The friction dissipation effects, contact conditions, and delamination growth phenomenon at delaminated interfaces and edges are overlooked. In order to demonstrate the capabilities of the developed formulation in predicting stability behavior of the thin-walled VSCL structures, some representative results are obtained and compared with those in the literature wherever available. The effects of material lay-ups, cutout size, delamination region and position on the stability of structure are studied. The accuracy and efficiency of the B-spline FSM calculation on the stability boundaries of perforated delaminated VSCL curved panels is shown through some different verification case studies. It is shown that the panels with larger cutout area have lower natural frequencies. This behavior is not observed for the fundamental frequency in case of panel with cutout edge ratio of 0.4. Additionally, for a perforated panel with edge delamination, it is shown that the delaminations of size smaller than delamination edge ratio of 0.2 has nearly no effect on the dynamic stability but the larger delamination sizes reduce the instability frequencies. It is also shown that the location of delamination occurrence in panel thickness direction weakly affects the fundamental vibration frequency but has considerable effects on the load bearing of the structure. For the case with fixed mid length fiber orientation on 45 degrees, higher orientation angles at the two ends makes the panel more stable. Finally, the stronger stability behaviors are observed in case of cylindrical panels with lower radius of curvature.

## References


Akhavan, H. and Ribeiro, P. (2011), "Natural modes of vibration of variable stiffness composite laminates with curvilinear fibers", *Compos. Struct.*, **93**(11), 3040-3047.

Hirwani, C.K., Patil, R.K., Panda, S.K., Mahapatra, S.S., Mandal, S.K., Srivastava, L. and Buragohain, M.K. (2016), "Experimental and numerical analysis of free vibration of delaminated curved panel", *Aerosp. Sci. Technol.*, **54**, 353-370.

Hyer, M. and Lee, H. (1991), "The use of curvilinear fiber format to improve buckling resistance of composite plates with central circular holes", *Compos. Struct.*, **18**(3), 239-261.

Hu, N., Fukunaga, H., Kameyama, M., Aramaki, K. and Chang, F.K. (2002), "Vibration analysis of delaminated composite beams and plates using a higher-order finite element", *Int. J. Mech. Sci.*, **44**(7), 1479-1503.

Ju, F., Lee, H.P. and Lee, K.H. (1995), "Free vibration of composite plates with delaminations around cutouts", *Compos. Struct.*, **31**(2), 177-183.

Kumar, A. and Shrivastava, R.P. (2005), "Free vibration of square laminates with delamination around a central cutout using HSDT", *Compos. Struct.*, **70**(3), 317-333.

Fazilati, J. (2017), "Stability analysis of variable stiffness composite laminated plates with delamination using spline-FSM", *Latin Am. J. Solids Struct.*, **14**(3), 528-543.

Fazilati, J. and Ovesy, H.R. (2013), "Parametric instability of laminated longitudinally stiffened curved panels with cutout using higher order FSM", *Compos. Struct.*, **95**, 691-696.

Mohanty, J., Sahu, S.K. and Parhi, P.K. (2015), "Parametric instability of delaminated composite plates subjected to periodic in-plane loading", *J. Vib. Con.*, **21**(3), 419-434.

Noh, M.-H. and Lee, S.-Y. (2014), "Dynamic instability of delaminated composite skew plates subjected to combined static and dynamic loads based on HSDT", *Compos. Part B*, **58**, 113-121.

Ovesy, H.R. and Fazilati, J. (2012), "Buckling and free vibration finite strip analysis of composite plates with cutout based on two different modeling approaches", *Compos. Struct.*, **94**(3), 1250-1258.

Ovesy, H.R., Fazilati, J. and Mahmoudabadi, M.R. (2014), "Finite strip buckling and free vibration analysis of laminated composite plates containing delamination using a first order layerwise theory", In: (B.H.V. Top-ping, P. Iványi Editors), *Proceedings of the Twelfth International Conference on Computational Structures Technology*, Civil-Comp Press, Stirlingshire, UK, Paper 24. DOI: 10.4203/ccp.106.24

Park, T., Lee, S.-Y. and Voyiadjis, G.Z. (2009), "Finite element vibration analysis of composite skew laminates containing delaminations around quadrilateral cutouts", *Compos. Part B*, **40**(3), 225-236.

Parhi, P.K., Bhattacharyya, S.K. and Sinha, P.K. (2001), "Hygrothermal effects on the dynamic behavior of mul-tiple delaminated composite plates and shells", *J. Sound Vib.*, **248**(2), 195-214.

Ribeiro, P., Akhavan, H., Teter, A. and Warmiński, J. (2014), "A review on the mechanical behaviour of curvi-linear fibre composite laminated panels", *J. Compos. Mater.*, **48**(22), 2761-2777.

Sahu, S.K. and Datta, P.K. (2002), "Dynamic stability of curved panels with cutouts", *J. Sound Vib.*, **251**(4), 683-696.

Sivasubramonian B., Rao G.V. and Krishnan A. (1999), "Free vibration of longitudinally stiffened curved panels with cutout", *J. Sound Vib.*, **226**(1), 41-55.

Sofiyev, A.H. and Kuruoglu, N. (2015), "Parametric instability of shear deformable sandwich cylindrical shells containing an FGM core under static and time dependent periodic axial loads", *Int. J. Mech. Sci.*, **101-102**, 114-123.

Sofiyev, A.H., Zerin, Z., Allahverdiev, B.P., Hui, D., Turan, F. and Erdem, H. (2017), "The dynamic instability of FG orthotropic conical shells within the SDT", *Steel Compos. Struct., Int. J.*, **25**(5), 581-591.

Sofiyev, A.H., Keskin, E.M., Erdem, H. and Zerin, Z. (2003), "The buckling of an orthotropic cylindrical thin shell with continuously varying thickness under a dynamic loading", *Indian J. Eng. Mater. Sci.*, **10**, 365-370.

Tornabene, F., Fantuzzi, N. and Bacciocchi, M. (2016), "Higher-order structural theories for the static analysis of doubly-curved laminated composite panels reinforced by curvilinear fibers", *Thin-Wall. Struct.*, **102**, 222-245.

Yang, J. and Fu, Y. (2007), "Analysis of dynamic stability for composite laminated cylindrical shells with delaminations", *Compos. Struct.*, **78**(3), 309-315.


*CC*